Spatiotemporal validation of IASI trace gas measurements at the pixel scale

O3M-SAF Visiting Scientist

Final Report

Mark A. Zondlo
Associate Professor, Princeton University
O3M-SAF Visiting Scientist

Satellite Application Facility on Ozone and Atmospheric Chemistry Monitoring (O3M SAF) of the European Organization for the Exploitation of Meteorological Satellites (EUMETSAT)

OM3SAF VS contact information:
Service de Chimie Quantique et Photophysique C. P. 160/09
Université de Libre Bruxelles
télé: (+32) 02 650 24 14
Campus du Solbosch
CP160/09, avenue F.D. Roosevelt 50, 1050 Bruxelles
Bldg. D: 109, DC7
Email: mzondlo@princeton.edu

VSA Supervisors:
Cathy Clerbaux, LATMOS/CNRS/Université Pierre et Marie Curie
Pierre-François Coheur, Université Libre de Bruxelles

Submitted to:
Seppo Hassinen
Finnish Meteorological Institute
P.O.BOX 503
FIN-00101 Helsinki
Finland

Tel: +358 50 409 7721
Fax: +358 9 1929 3146
seppo.hassinen@fmi.fi

October 3, 2016

Table of Contents

1. Introduction

The overall goal of this project was to validate trace gas measurements from IASI at the pixel scale over a range of environments and timescales. IASI measurements were compared to those derived from in-situ measurements from multiple aircraft-, vehicle-, radiosonde-, and network-based field experiments. Validation of column abundances of carbon monoxide (CO), ozone (O_3), sulfur dioxide (SO_2), nitric acid (HNO_3), and ammonia (NH_3) were examined at narrow spatial (15-200 km) and temporal (0.5-3 hours) windows. These trace gas species are the four products generated in the framework of CDOP2/O3MSAF and one future prospect (NH_3). While validations for CO and O_3 have been conducted in the past,[1,2] the unique aspects of this study were the narrow spatiotemporal windows at which the validations were conducted (~10-100 minutes, ~10-100 km) and the development of methods to validate for short-lived species (in this case using NH_3, a trace gas critically linked to the formation of unhealthy particulate matter).

1.1 Key in-situ dataset: NASA DISCOVER-AQ Colorado / NSF FRAPPE

The key in-situ datasets used for in-situ/IASI validation were from the field experiments of NASA DISCOVER-AQ Colorado (Deriving Information on Surface Conditions from COlumn and VERtically Resolved Observations Relevant to Air Quality, DISCOVER-AQ)[3] and NSF Front Range Air Pollution and Photochemistry Experiment (NSF FRAPPE).[4] These field experiments had the most comprehensive set of measurements for satellite intercomparisons because the two field studies occurred in the same region, timeframe, and in a coordinated manner. Because the amount of in-situ and satellite data within narrow spatiotemporal windows (~ hour, ~ 10s of km) were very limited, the DISCOVER-AQ Colorado / NSF FRAPPE field study provided the most robust dataset to conduct the validations and is the focus of the validation efforts as opposed to other DISCOVER-AQ field sites (Texas, California).

For example, Figure 1 shows the flight tracks of the a) NASA P-3B aircraft, b) NSF C-130 aircraft, and c) MetOp/A IASI NH_3 column abundances during the Colorado field experiments. Not shown are the plethora of ground-based stations and mobile laboratories that were also involved in this field study. The P-3B aircraft conducted repeated spirals between the near surface (0.1 km) and 5.5 km in altitude at fixed locations throughout the campaign. The measurements from these spirals were the primary data source for most of the validation studies. The C-130 examined horizontal gradients at select altitudes across the Colorado Front Range and adjacent plains. Mobile laboratories, balloonsondes, and ground-based sites provided additional validation data. The NASA DISCOVER-AQ field experiment in Colorado therefore provided excellent vertical and horizontal coverage of in-situ measurements for satellite validation studies.

1.2 Other datasets

Validations from DISCOVER-AQ Houston (Sept. 2013) and DISCOVER-AQ California (San Joaquin Valley, Jan./Feb. 2013) are also reported where significant differences exist from the Colorado data. Surface measurements were also analyzed during the 2013 and 2014 Campaigns of Air Quality Research in Beijing and Surrounding Regions (CAREBEIJING-NCP),[2] but because no vertical profiles (flight data) were conducted, this dataset had limited utility.
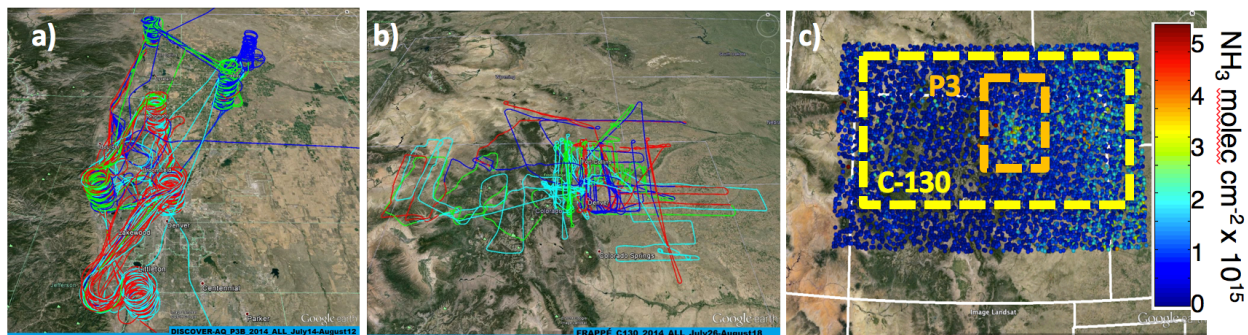
Fig. 1: Data coverage in the NASA DISCOVER-AQ Colorado / NSF FRAPPE field study showing (a) NASA P-3B flight tracks, (b) NSF C-130 flight tracks, and (c) IASI NH_3 column abundances from MetOp/A (dashed boxes represent the approximate size of flight domains of the P-3 and C-130). IASI shows relatively high NH_3 columns where the intensive airplane sampling occurred, a region of high agricultural as well as urban emissions.

2. Work Packages

A description of the activities for each of the work packages are noted below. Note that additional analyses since the original submission of Work Package #1 have been included and updated in this report.

WP 1: Validation of IASI column abundances

CO intercomparisons

IASI column CO profiles were compared to the NASA P-3B aircraft spirals. The in-situ CO measurements were made by the NASA DACOM instrument (PI: Glenn Diskin). The accuracy of the in-situ measurement was the greater of 2% or 2 ppbv. The geographic mean and mean time of the aircraft spiral profiles were compared to the IASI centroid location and time. A total of 169 datapoints fit within a spatial window of ±60 km and temporal window of ±2 hours. Note that the P-3B aircraft's typical flight ceiling of ~ 5.5 km in altitude limited direct comparisons from the surface (generally 1.5-2 km in Colorado) to this altitude.

Figure 2a shows a comparison of the mean aircraft (blue) and IASI CO (red) vertical profiles binned every km from 1-6 km. Figure 2b shows the mean values (±1σ) of each bin during the Colorado field studies. Overall, IASI CO read 7% higher than the in-situ measurements and both were within the variability of each other. IASI read 12% lower than the aircraft data in the lowermost boundary layer (1-2 km). For other altitudes, the relative agreement was -1% (2-3 km), 14% (3-4 km), 17% (4-5 km), and 17% (5-6 km).

O_3 intercomparisons

IASI O_3 profiles were compared with ozonesondes (launch location and time) and in-situ aircraft profiles (center location and time) within two hours and ±60 km of the IASI centroid/overpass time. Ozonesonde data (10% accuracy) were from Anne Thompson at Pennsylvania State University, and aircraft O_3 data (5% + 0.1 ppbv accuracy) were from Andy Weinheimer (NCAR). There were 179 IASI measurements that had in-situ profiles within these spatial and temporal constraints. In-situ data were averaged within the corresponding vertical IASI window (from the surface to the nearest integer kilometer above sea level and then in 1 km bins thereafter). Figure 3a shows the profiles from IASI (red) and in-situ (blue) measurements for Colorado, and Figure 3b shows the relative error with respect to the in-situ measurements. IASI
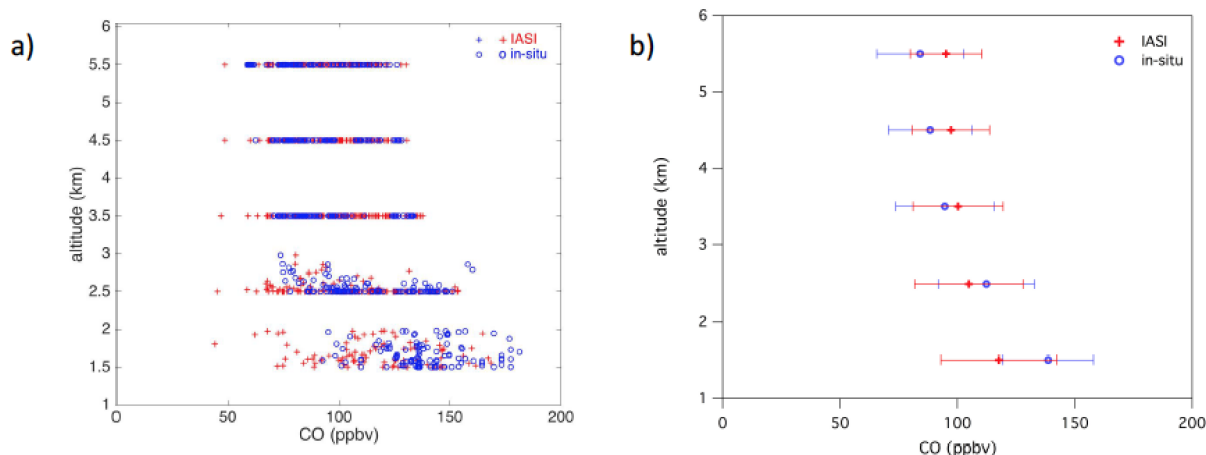
Fig. 2: a) IASI (red) and aircraft (blue) data binned within 1 km increments (N=169 points) for data within ±2 hours and ±60 km of the IASI overpass time and location. b) Mean and standard deviation of the data in (a). Over this altitude range, IASI read 7% higher than the in-situ data, within the combined uncertainties of both measurements.

underestimates O_3 nearest the surface by nearly 50% but generally agrees well with in-situ data from the upper troposphere (~ ±10%) and from 20-30 km (~ ±5%). The lower tropospheric differences cannot be explained by uncertainties in the IASI profiles (generally ~20% in this region) or in the in-situ measurements (10%). Deviations near the tropopause are most likely related to slight differences in the actual versus retrieved tropopause height where large gradients in ozone maximize.

SO₂ intercomparisons

Sulfur dioxide was not measured on either aircraft in Colorado, nor was it measured in the other DISCOVER-AQ campaigns. No vertical profiles were conducted in CAREBEIJING, either. For this reason, no comparisons were able to be conducted with IASI.
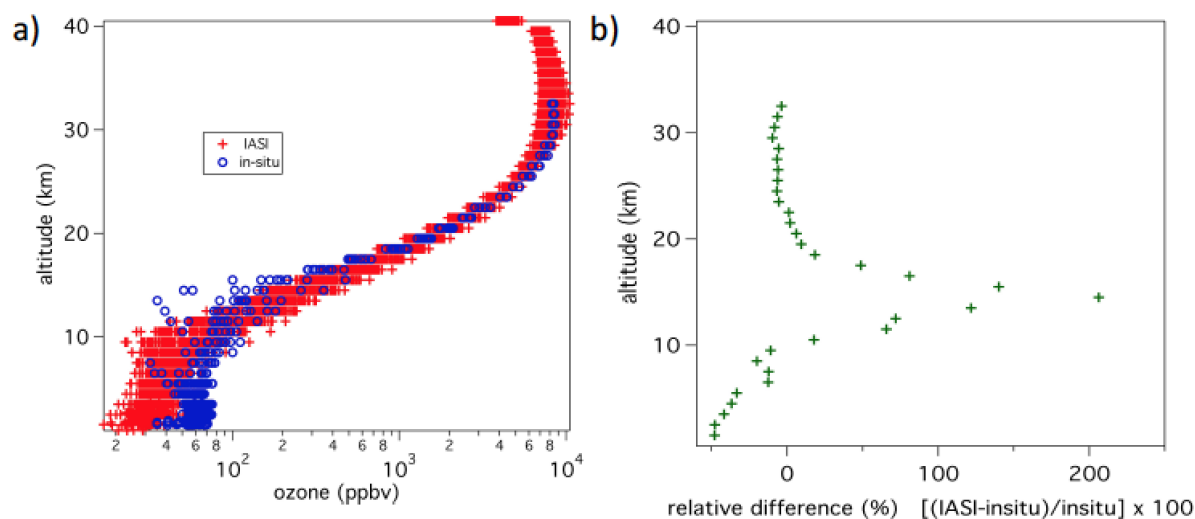

Fig. 3: a) Ozone from IASI (red) and ozonesondes (blue) for 1 km vertical bins where the mean sonde location and time was ±2 hours and ±60 km of the IASI overpass time and centroid. b) relative differences between IASI and the ozonesonde for each altitude bin.

HNO₃ intercomparisons

HNO$_3$ intercomparisons

Figure 4 shows box-whisker plot profiles from DISCOVER-AQ Colorado (a), Texas (b), and California (c). In all three cases, the median integrated HNO$_3$ column amounts derived from the aircraft data for each campaign were < 1.5 x 10^{15} molec cm^{-2}. Typical IASI HNO$_3$ columns were at least an order of magnitude larger than these in-situ amounts, and therefore the lower half of the troposphere contributes negligibly to the overall HNO$_3$ column. A case study on July 28, 2014, in Colorado examined whether the assumption of uniform HNO$_3$ in the stratosphere over small scales (e.g. field study domain) could yield differences in the boundary layer HNO$_3$. Unfortunately, the overall IASI HNO$_3$ column variability over the range of 1.02-1.70x10^{16} molec cm^{-2} showed no spatial correlation to the aircraft-derived column amounts of 0.7-1.2x10^{15} molec cm^{-2}. For these reasons, no further validations of IASI HNO$_3$ was conducted.
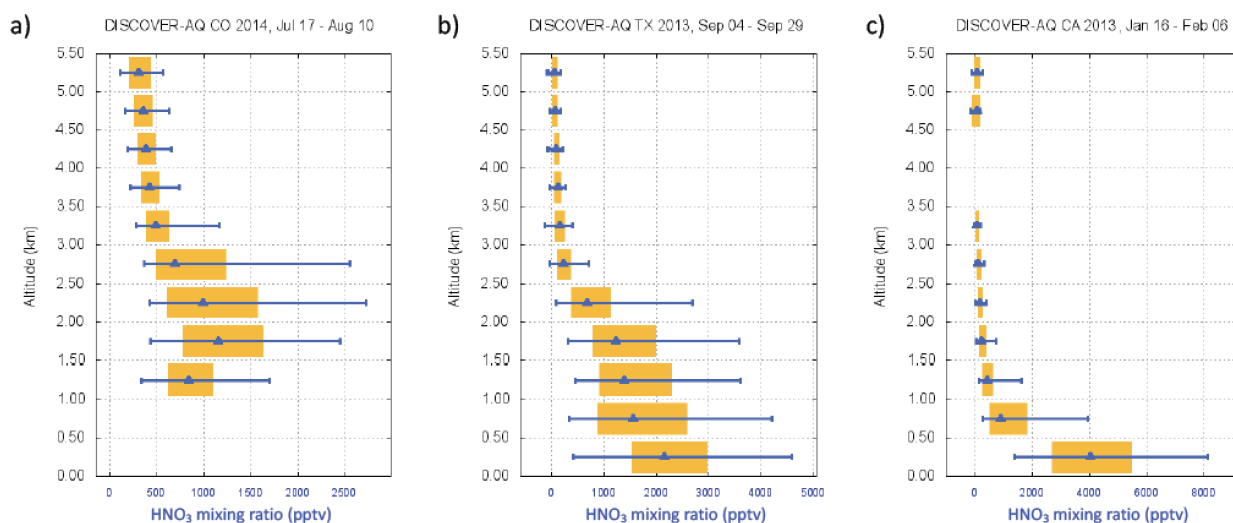

Fig. 4: Vertical profiles of HNO$_3$ in DISCOVER-AQ Colorado (a), Texas (b), and California (c). The column amounts of HNO$_3$ up to the altitude ceiling of 5.5 km was negligible to the overall IASI HNO$_3$ columns due to the much larger stratospheric HNO$_3$ abundance.

NH$_3$ intercomparisons

The first progress report focused on IASI NH$_3$ measurements from MetOp/A with the look up table (LUT) algorithm[5] during the NASA DISCOVER-AQ Colorado campaign in summer 2014. We present updated results in this section with three improvements since that first progress report: 1) IASI NH$_3$ column abundances with a neural network retrieval algorithm[6] that has significant improvements over the prior LUT algorithm, particularly in removing positive biases; 2) inclusion data from both MetOp/A and /B satellites (only MetOp/A was shown previously); and 3) inclusion of data from the NSF FRAPPE study in Colorado in summer 2014 as well as the NASA DISCOVER-AQ California study in the San Joaquin Valley of California, USA, in winter 2013. Note that no airborne-based measurements of NH$_3$ were taken in the other available datasets (NASA DISCOVER-AQ Houston, NASA DISCOVER-AQ Washington-Baltimore, CAREBEIJING 2013 and 2014), and thus no intercomparisons were conducted for these campaigns.

Because of the short-lived nature of NH$_3$ (hours to days atmospheric lifetime) compared to the other species above, it was necessary to use a narrower spatiotemporal window of ±15 km and

±60 minutes from the IASI overpass/centroid. Note this window is comparable in space and time with a mean boundary layer wind speed of ~ 4 m s^{-1}. A total of N=89 columns were constructed within this spatiotemporal window. Data were analysed by two methods: 1) an orthogonal linear regression of IASI vs. in-situ data; and 2) a Gaussian fit to the residuals of IASI minus the in-situ data. The first method yields information on the correlation, slope, and offset but can be strongly driven by outliers. In contrast, a Gaussian fit to the histogram of the differences is less influenced by outliers but with limited information on the reason for the disagreement (whether due to an offset or a slope). Both datasets were filtered to remove any points with relative error greater than 100% and an absolute error >3x10^{15} molec cm^{-2}. In this way, it was possible to examine agreement at relatively low column amounts where relative noise may be large but absolute noise is still fairly small.

For relatively low/moderate NH$_3$ column amounts of <10^{16} molec cm^{-2} (the mean column amount overall was 6.0x10^{15} molec cm^{-2}), a total of 69 matches yielded a correlation coefficient of 0.36 with IASI reading lower than the in-situ columns by about 30%. These are the first validations of any satellite data at such low (clean) column amounts. However, it was noticed that the air temperatures retrieved by the MetOp satellites often did not represent those within the boundary layer from nearby soundings. Table I shows how the agreements in the slope, correlation coefficient, intercept and difference between the peak of the histogram and in-situ values all improved as the MetOp temperature more closely represented the actual air temperature at the surface.

T$_{diff}$ (K)	N	r	m	b	peak historgram	mean in-situ
<20	69	0.36	1.88	-8e15	-2.6e15	6.0e15
<10	57	0.39	1.68	-6e15	-2.3e15	5.8e15
<5	20	0.42	1.25	-4e15	-2.2e15	5.5e15
<2.5	10	0.68	0.79	-1e15	-2.0e15	5.5e15

Table I: Sensitivity of the agreement to differences in the surface air temperature between IASI and nearby radiosondes (T$_{diff}$). While the number of matches (N) decreases, the correlation coefficient (r), slope (m), and intercept (b) of an orthogonal linear fit all improve significantly. In addition, the peak of a Gaussian fit to the histogram of the IASI-(in-situ) differences also improves with better surface air temperature agreement. All data were for in-situ columns < 10^{16} molec cm^{-2} and when the absolute error was <3x10^{15} or the relative error was <100%.

For all NH$_3$ column amounts (restricted to temperature differences < 5 K between the IASI and observed surface air temperature), IASI showed a progressively larger negative bias as the in-situ NH$_3$ columns increased. Figure 5 shows a plot of the difference of IASI and in-situ columns versus the in-situ column amounts. While agreement is surprisingly good at the very small column amounts, there is a large difference at very high NH$_3$ columns. Ongoing efforts are investigating the causes of this apparent low bias in IASI at high column amounts. One potential reason could be biases in the in-situ measurements themselves; at very large NH$_3$ concentrations, in-situ instruments have outgassing of adsorbed NH$_3$ onto instrument/inlet surfaces.[7] Therefore, an aircraft going from a very polluted boundary layer into the free troposphere would result in an artificially biased high measurement as adsorbed NH$_3$ goes into the sampling system. Improved in-situ measurements of NH$_3$ may be needed to fully address this apparent discrepancy between IASI and in-situ measurements at high column amounts.
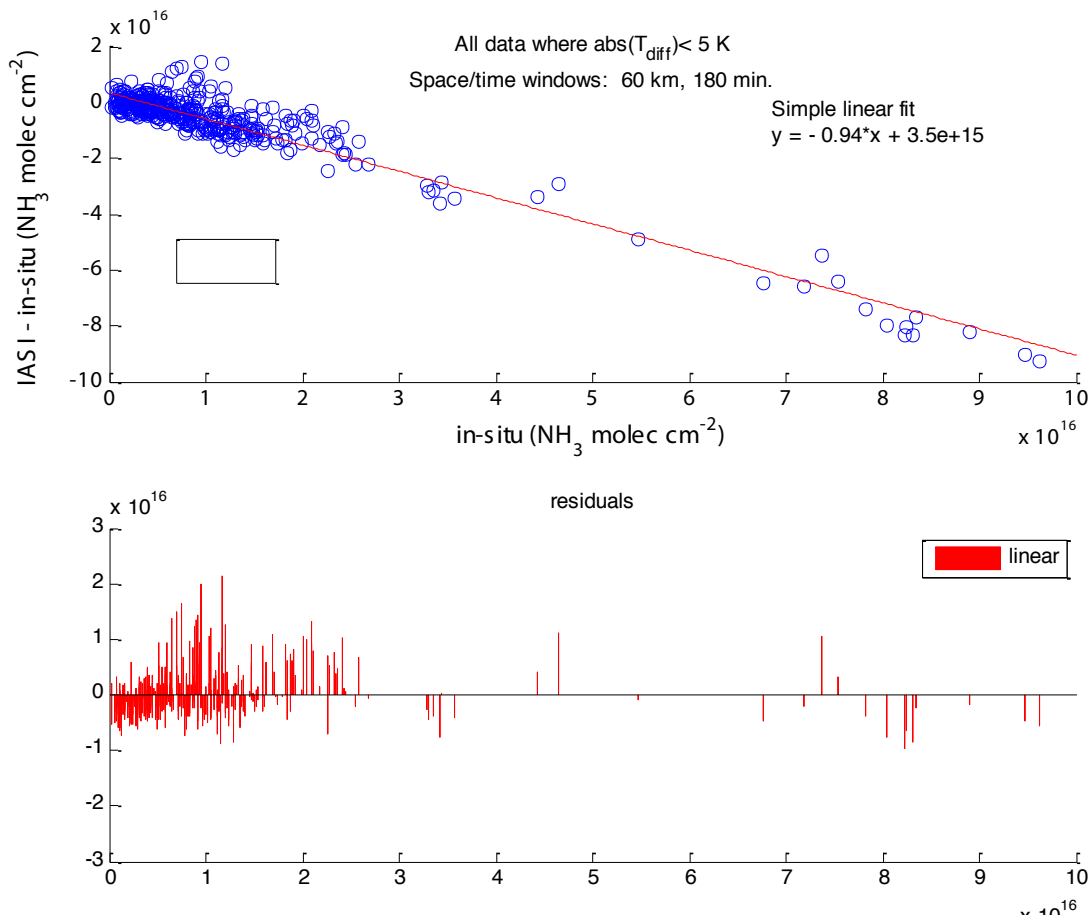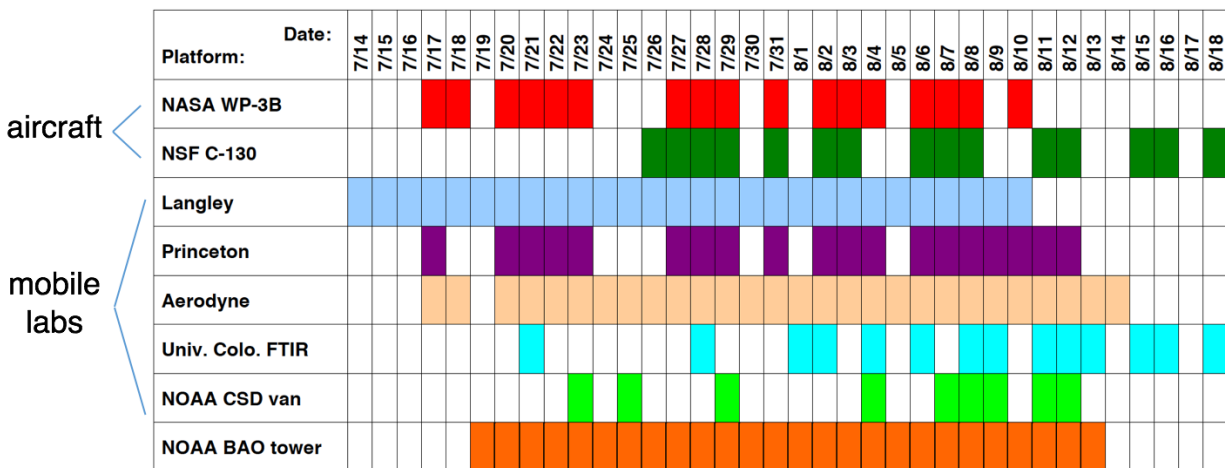
Fig. 5: Plot of IASI minus in-situ NH_3 column abundances versus the in-situ column (top) and the residuals from the linear fit (bottom). A strong dependence is observed where IASI reads much lower than the in-situ measurements at high NH_3 column amounts. The reason for this discrepancy is not clear but may be related to sampling artifacts in the in-situ measurements themselves from instrument/inlet outgassing when sampling the polluted boundary layer and then going into the cleaner, free troposphere.

Status: This task has been completed.

Work Package 2: Intra- and inter-pixel spatial variability

The focus of this task was on the development of methods to examine how to validate a short-lived tracer at the pixel scale and to identify potential issues in both the sampling and interpretation of comparisons. For these studies, we selected NH_3 due to its short lifetime and extreme heterogeneity in space (cf. O_3 (weeks) and CO (months) are long-lived gases in the troposphere compared to NH_3). In addition to the aircraft NH_3 measurements which contributed to the majority of the construction of the in-situ profiles described previously, the Colorado field study had a plethora of in-situ surface NH_3 measurements including several mobile laboratories, and a carriage on a tower that profiled continuously between the surface and 100 m above ground. Table II shows the suite of NH_3 measurements that were used to examine spatial variabilities, particularly on the pixel scale.

8

In-situ NH₃ measurements

aircraft
- NASA WP-3B
- NSF C-130

mobile labs
- Langley
- Princeton
- Aerodyne
- Univ. Colo. FTIR
- NOAA CSD van
- NOAA BAO tower

Date (columns): 7/14, 7/15, 7/16, 7/17, 7/18, 7/19, 7/20, 7/21, 7/22, 7/23, 7/24, 7/25, 7/26, 7/27, 7/28, 7/29, 7/30, 7/31, 8/1, 8/2, 8/3, 8/4, 8/5, 8/6, 8/7, 8/8, 8/9, 8/10, 8/11, 8/12, 8/13, 8/14, 8/15, 8/16, 8/17, 8/18

Sondes for pressure, temp. profiles (A. Thompson, Penn State; Erik Olson, Univ. Wisconsin)

NH₃ measurements during DISCOVER-AQ/FRAPPE in Colorado:

platform	avg. uncertainty	method	PI
P3-B	30%	PTRMS	A. Wisthaler (Innsbruck)
C-130	34% + 0.39 ppbv	TDL	J. Nowak (Aerodyne)
Aerodyne mob.	34% + 0.39 ppbv	TDL	C. Floerchinger (Aerodyne)
Princeton mob.	20% + 0.4 ppbv	Open-path	M. Zondlo (Princeton)
CU column	10%	FTIR	R. Volkamer (CU)
NOAA/CSD	20% + 0.3 ppbv	Picarro	A. Neuman (NOAA CSD)
NOAA/BAO	20% + 0.3 ppbv	Picarro	J. Murphy (Univ. Toronto)

Table II: Ammonia measurements in the NASA DISCOVER-AQ/NSF FRAPPE field experiments in Colorado. The P-3B and C-130 are aircraft measurements while the next five are mobile laboratories. The last one is an in-situ measurement on a tower that profiled the lowermost 100 m. The Langley mobile laboratory, though not measuring NH₃, made aerosol composition measurements including NH₄⁺ which can aid in the interpretation of phase partitioning.

Another reason for the potential disagreement in the NH₃ column amounts between IASI and in-situ measurements, particularly at high column abundances, may be the strong spatial gradients of NH₃. Figure 6 shows NH₃ concentration gradients in DISCOVER-AQ California from the Princeton mobile laboratory.[8] With a prevailing wind from the southeast, anytime the mobile laboratory drove downwind of an agricultural feedlot (shown as a white dot in Fig. 6), NH₃ increased by one to two orders of magnitude. The extent to which such strong gradients are

Fig. 6: NH₃ spatial heterogeneity in the San Joaquin Valley in California. White dots represent feedlots.

captured by IASI would significantly impact the overall agreement. Indeed, Figure 7 shows an interpolated/averaged map of the southern San Joaquin Valley from the same mobile laboratory
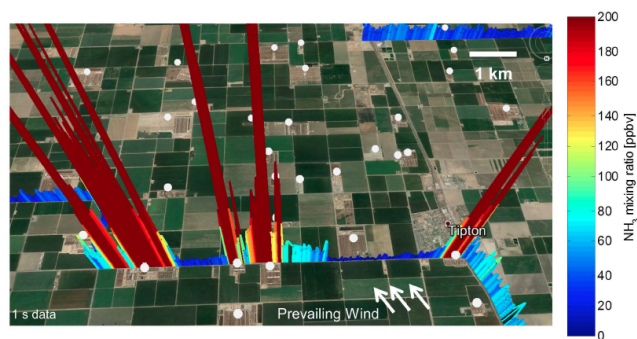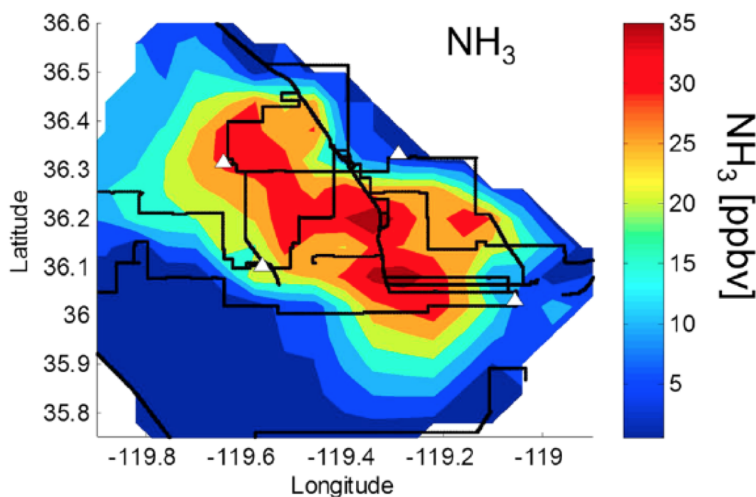
Fig. 7: Interpolated/averaged NH$_3$ from the mobile laboratory in the southern San Joaquin valley of California. The concentrations even at this broader scale (~ 80 km across) still show strong spatial gradients.

where individual feedlots/farms no longer are visible. This perhaps would be more representative of what a satellite would see in this region.

Figure 8 shows another case study of intrapixel variability and how it may play a role in uncertainties in the comparison of aircraft and IASI measurements. Panel (a) represents the IASI centroid and ellipse and the locations of the various in-situ measurements. The 15 km radius from the IASI centroid is shown in light blue and is the spatial averaging window for this comparison. Pink is the NASA P-3B aircraft, blue is the NSF C-130 aircraft, and yellow is the University of Colorado mobile FTIR. Panel (b) shows the same view but this time colored by altitude. The P-3B aircraft is spiraling upward within the IASI ellipse. Meanwhile, the C-130 aircraft was at constant altitude and the mobile FTIR also was at nearly constant altitude on the ground. Panel (c) shows the MetOp/B temperature vertical profile and that of the nearest radiosonde (Penn. State Univ.). Panel (d) shows the vertical profile of NH$_3$ from the P-3B (pink) and C-130 (blue). Note near the ground there is a wide range of concentrations. An average profile is shown by the black line with a bin within 100 m of the ground, followed by 500 m bins thereafter above it. Thin lines on either side of the vertical profile represent the variability within each bin. Panel (e) shows the NH$_3$ concentration versus time colored by altitude. If one looks at the dark blue line (nearly constant altitude), one observes significant variation in NH$_3$ over this two-hour window. Also shown in Panel (e) on the right axis is the NH$_3$ column versus time. Again, large variability is observed within a factor of three while driving across the IASI ellipse and spatial window. Finally, Panel (f) shows an altitude-time plot with the P-3B clearly ascending in the spiral. The large "+" symbols in panels (e) and (f) are the time of the IASI overpass.

The IASI measurement in this pixel was 4.6 ($\pm$1.5) x 10^{15} molec cm^{-2} whereas the in-situ derived column was much higher at 2.3x10^{16} molec cm^{-2} (assuming no NH$_3$ above the highest measurement). The CU mobile FTIR was also closer to the in-situ derived column at 1.0 x 10^{16} molec cm^{-2}, though there is large variability along its transect over a very short distance (~ 25 km). Therefore, in a highly heterogeneous NH$_3$ source region such as Colorado, large intrapixel gradients will exist that can greatly influence the comparisons.

To this end, the agreement between IASI and in-situ measurements were compared across a range of spatial and temporal windows for NH$_3$. Spatial windows varied from inside the IASI ellipse only to $\pm$60 km, and temporal windows were varied from $\pm$20 to $\pm$180 minutes. Figure 9 shows the results of an orthogonal linear regression for the (a) number of points, (b) correlation

coefficient and (c) slope of the fit versus various space/time windows. Note that a spatial window of "zero" is equivalent to all in-situ data being inside the ellipse. Overall, there is improvement in the correlation coefficient and slope at smaller space and time windows. Spatial windows play a stronger role in the agreement than temporal windows. However, there is a data limit to which the spatial and temporal windows can be narrowed; at very tight space/time windows, there is a paucity of data to which one can intercompare.

In summary for this work package, it is absolutely critical to consider intrapixel and interpixel variability when validating short-lived species. While areas with a homogeneous concentration field may seem like ideal sites for future validations, by its nature a homogeneous concentration field is likely far from any sources and therefore likely to be at lower concentrations. Clearly, some of the good agreement at low column amounts in Fig. 5 may very well be due to the presence of a more uniform NH_3 field, whereas at higher column amounts, spatial heterogeneities dominate the column and hence agreement. If high-resolution spatial spikes of NH_3 as shown in Figs. 5, 6, and 7e cannot be resolved by the satellite, this could be another potential reason for the larger disagreements (and progressively worse low bias) at higher column amounts.
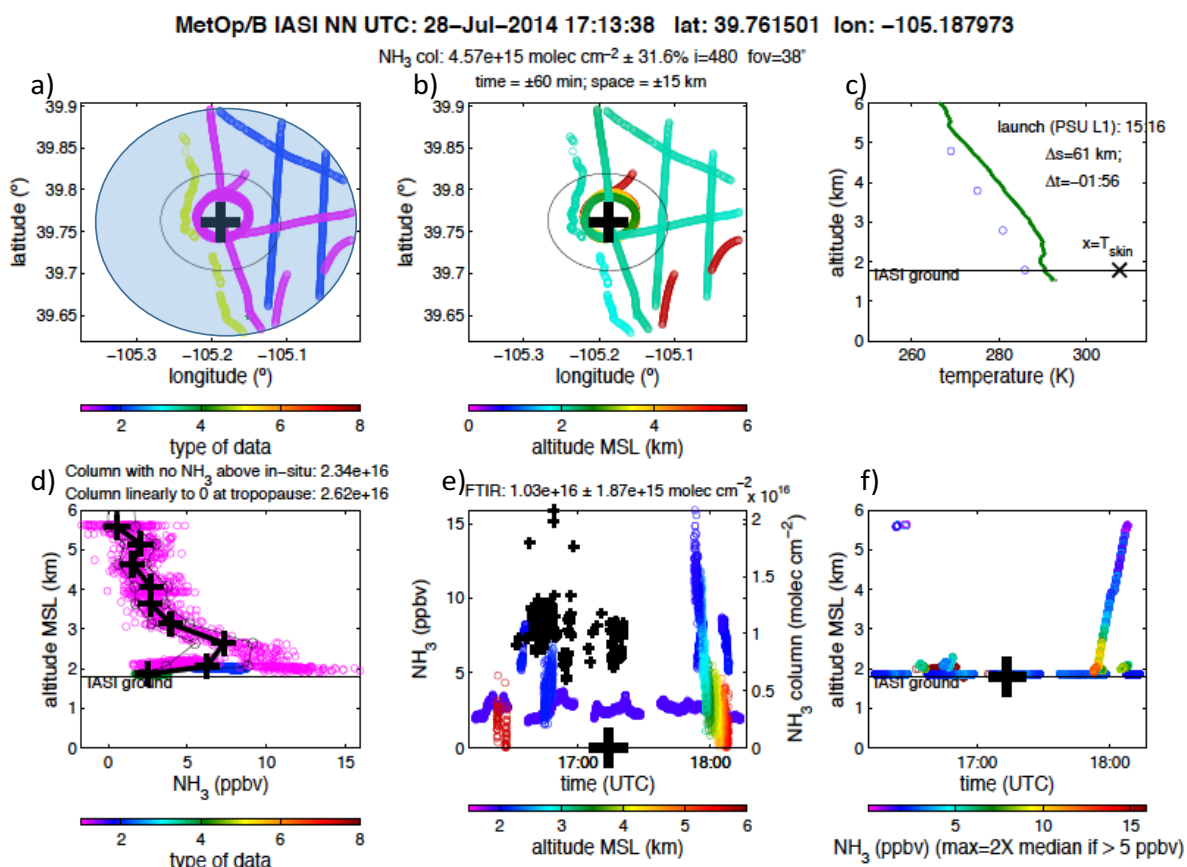

Fig. 8: a) IASI ellipse and spatial window (blue) with P-3B aircraft flight tracks (pink), C-130 aircraft (blue), and CU FTIR mobile lab (yellow). b) Same as (a) but colored by altitude. c) Temperature profile from MetOp/B and nearby sonde. d) In-situ derived vertical profile of NH_3 colored by aircraft. e) Timeseries of NH_3 concentration (left) and CU FTIR NH_3 column (right). f) Timeseries of altitude for each measurement.
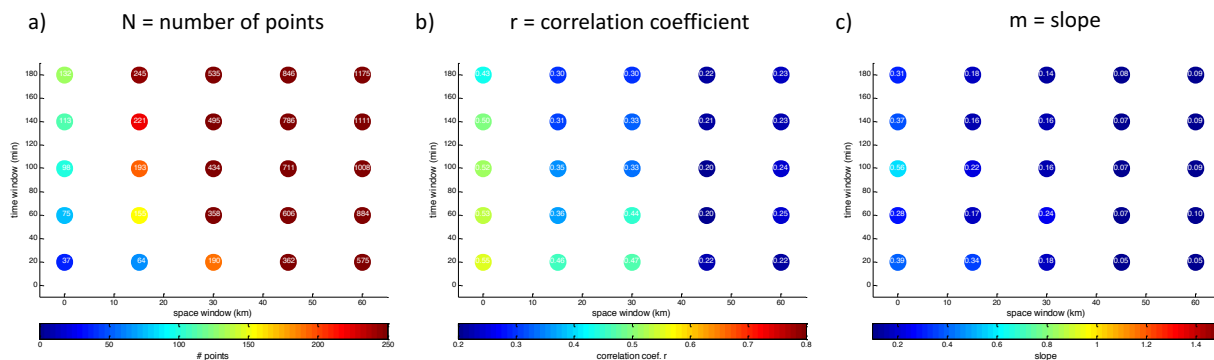
11

Fig. 9: Space/time window versus a) number of datapoints, b) correlation coefficient, and c) slope of orthogonal linear regression for all $_{NH3}$ data (no error, concentration, or surface temperature filter). Improved agreement is seen at smaller spatial and temporal windows, with a stronger effect being the spatial window.

Status: WP2 has been completed.

Work Package 3: Temporal variability at non-overpass times

This work package focuses on the representativeness of the morning overpass compared to other times of the day. Figure 10 shows three aircraft NH_3 profiles over an agricultural area (Platteville, Colorado) taken at 14:20, 16:37, and 20:06 UTC. For reference, the IASI overpass occurred at 16:24 UTC, almost the same time as the middle panel in Fig. 10. About two hours prior to the overpass, NH_3 shows a 55% lower column amount than near the overpass time. About three and a half hours after the overpass, the NH_3 column is about 20% higher than near the overpass time. Most of the differences in the column are occurring in the lowermost boundary layer, the closest few hundred meters to the ground (though the inversion height does increase during this time).

The diurnal cycle of ammonia fluxes was directly measured at a cattle feedlot in Colorado by the visiting scientist in 2013.[9] Figure 11 (a) shows how NH_3 shows a strong diurnal dependence that is correlated with the air temperature. Ammonia is volatilizing from surface waste that gets heated by the sun. In contrast, Fig. 11 (b) shows that CH_4 does not have a diurnal dependence and instead has some fluctuations that were more associated with animal feedings (but at a much lower variability/range than NH_3). The diurnal cycle of emissions is consistent with the observed in-situ aircraft profiles of NH_3.

Most directly comparable to the data in Fig. 10 (same year), Figure 12 shows diurnal measurements taken by various mobile laboratories of the NH_3:CH_4 ratio around feedlots in Colorado in 2014.[10] Because CH_4 emissions are expected to be roughly constant over the diurnal cycle (from animal respiration), the NH_3:CH_4 emission ratio is a proxy for NH_3 emissions from agricultural feedlots. The emission ratio shows a strong correlation with air temperature, consistent with volatilization of NH_3 from animal waste on the ground. The emission ratio increases most sharply in the early to mid-morning when temperature rises the fastest, again broadly consistent with the in-situ column measurements. Indeed, the increase between the 16:37
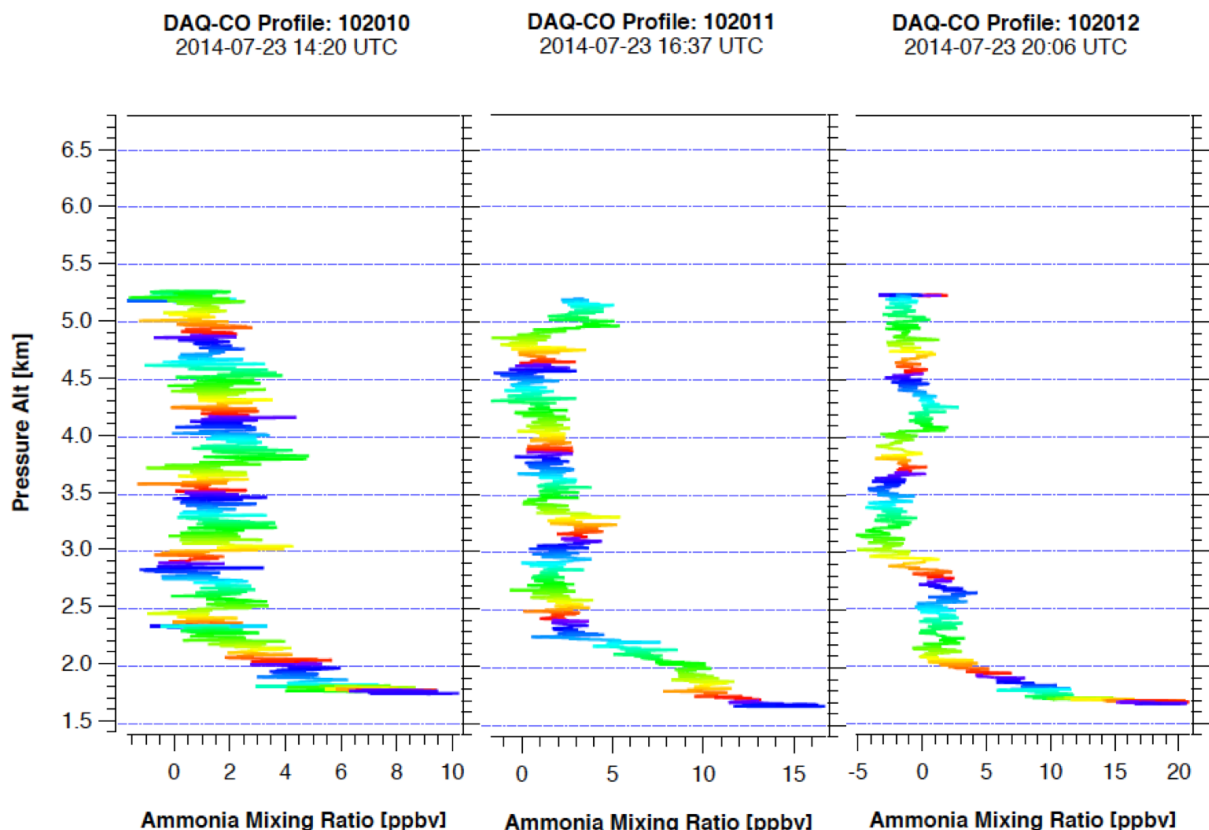
Fig. 10: Aircraft profiles of NH_3 at Platteville, Colorado, on July 23, 2014. The largest changes are in the lowermost surface layer with the column amounts increasing by 75% from 14:20 to 20:06 UTC (8:20-14:06 local). The IASI overpass on this day was at 16:24 UTC, nearly identical to the middle profile. The colors on the graphs are related to aircraft heading during the spiral and should be ignored.
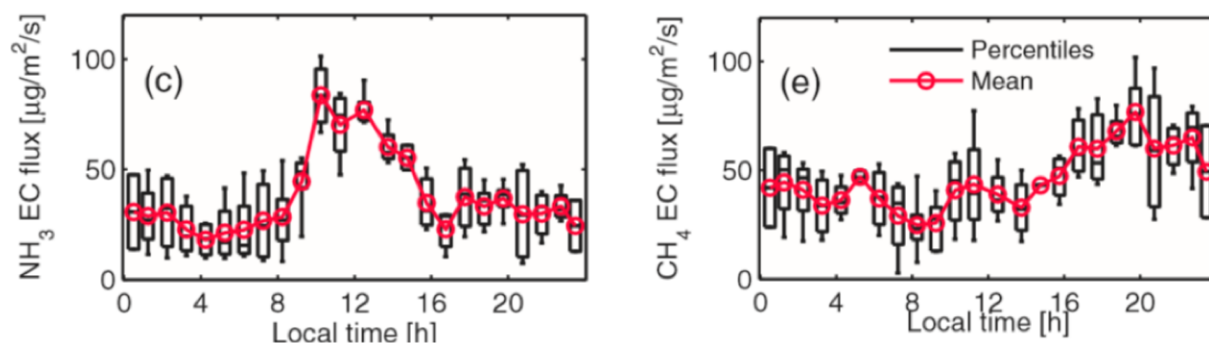

Fig. 11: Ammonia (left) and methane (right) fluxes at a cattle feedlot in Colorado made by the visiting scientist in November 2013. The NH_3 fluxes show a strong diurnal dependence, whereas the CH_4 is largely stable with little diurnal patterns. The methane fluxes are shown to help interpret the NH_3:CH_4 emission ratios during the Colorado campaign. From Sun et al. [2015].

and 20:06 UTC profiles (10:37-14:06 local) is   less than one from 14:20 to 16:37 (8:20-10:37 local).

These results suggest that in agricultural areas such as feedlots, the IASI column for the morning overpass could be scaled with the ambient temperature to derive columns for other times of the

day. Of course, the change of the boundary layer height also factors into the retrieved profile but should not impact the total column (all things being equal as the NH$_3$ would be distributed over a larger vertical area). One caveat, however, is that changes in temperature and humidity during this time may alter the partitioning between particulate ammonium and gas phase NH$_3$. Therefore, the NH$_3$ column may not show the same behaviour as the emissions themselves.
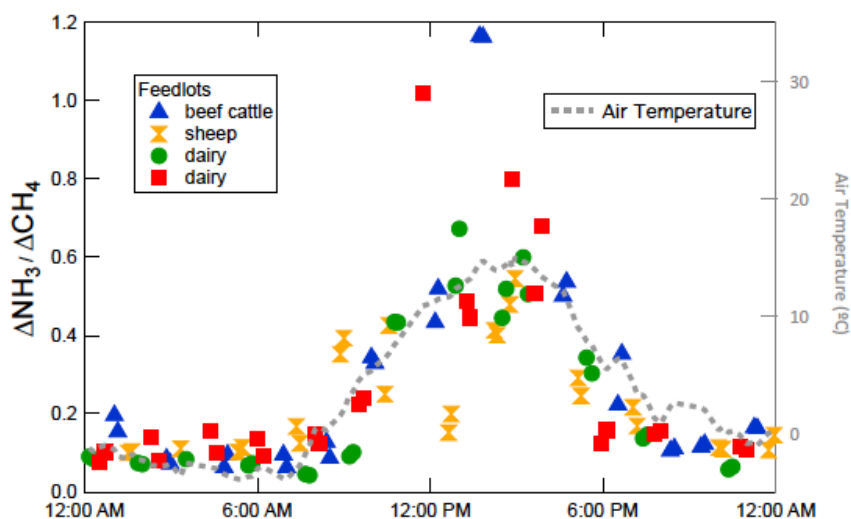

Fig. 12: Emission ratio of NH$_3$:CH$_4$ from a 3-day diurnal study taken by the NOAA Chemical Sciences Division (A. Neuman), Princeton, and Aerodyne mobile laboratories.

Finally, the aircraft profiles of O$_3$ and CO at different times of the day over Denver, Colorado, are shown in Fig. 13. This spiral was conducted over the middle of a large metropolitan (2.5 M people) area. For reference, the air temperature, potential temperature, and humidity profile are also shown. These profiles were taken during a vertical spiral on the aircraft on August 2, 2014, at 15:39, 18:05, and 21:15 UTC.

The earliest profile (Fig. 13a) shows high CO near the surface (250 ppbv) during the morning rush hour and before the inversion has fully broken. Above the surface layer, CO is closer to its background level of 100 ppbv. Ozone remains fairly low throughout the column with some evidence of destruction in the boundary layer (30 ppbv) and 60 ppbv above it. Photochemical smog production has not fully started.

At 18:05 UTC (12:05 local, Fig. 13b), the previously high concentrations of CO near the ground have mixed up through the boundary layer to a height of 2.7 km with a mean value around 140 ppbv. Ozone has gradually increased to 65-70 ppbv in the boundary layer.

By 21:15 UTC (Fig. 13c), CO levels from the surface to 4 km altitude are around 120 ppbv. The layer is thicker but at a lower concentration as before with some structure likely due to advection of different airmasses above Denver. Ozone continues to increase upward with values of 70-75 ppbv upward to 4 km altitude.

Because CO and O$_3$ have relatively long lifetimes, the changes in vertical profiles are not as sensitive as NH$_3$. While CO has local sources in urban areas (traffic), its background is sufficiently high that one mainly observes the lowering of concentrations as the boundary layer increases during daytime. Ozone is produced photochemically and peaks in the late afternoon based upon actinic flux, nitrogen oxides, and volatile organic carbon compounds. Overall, the changes in the vertical profiles of both species are based upon accurate knowledge of boundary layer height and atmospheric composition. As shown previously in Figs. 2 and 3, IASI captures the CO and O3 profiles with reasonable accuracy in the lower and middle troposphere.

14

Fig. 13: Timeseries of O$_3$ and CO profiles over Denver, Colorado.
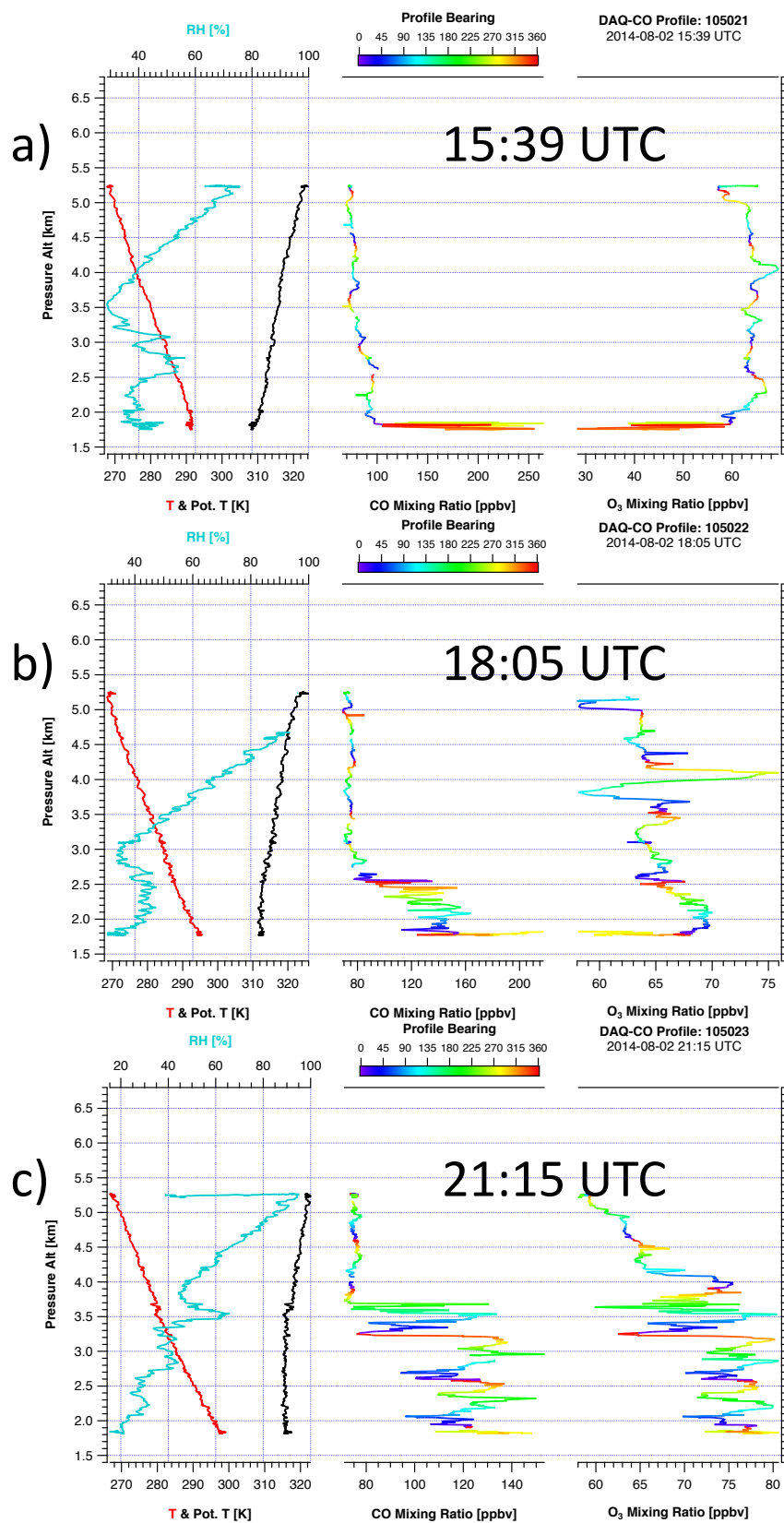
Status: WP3 has been completed.

4. Data availability

The NSF FRAPPE and DISCOVER-AQ field data are publically-available at the following website:

http://www-air.larc.nasa.gov/missions/discover-aq/discover-aq.html

This site links to the individual measurement files from every group during the combined Colorado campaigns (including NSF FRAPPE) as well as the DISCOVER-AQ studies in Texas, California, and the Mid-Atlantic.

5. References

1. Pommier, M., C. Clerbaux, K.S. Law, G. Ancellet, P. Bernath, P.-F. Coheur, J. Hadji-Lazaro, D. Hurtmans, P. Nédélec, J.-D. Paris, F. Ravetta, T.B. Ryerson, H. Schlager, and A.J. Weinheimer, A. J. (2012), "Analysis of IASI tropospheric O3 data over the Arctic during POLARCAT campaigns in 2008", *Atmos. Chem. Phys.*, *12*, 7371-7389, doi:10.5194/acp-12- 7371-2012.
2. Kerzenmacher, T., B. Dils, N. Kumps, T. Blumenstock, C. Clerbaux, P.-F. Coheur, P. Demoulin, O. Garcʹıa, M. George, D. W. T. Griffith, F. Hase, J. Hadji-Lazaro, D. Hurtmans, N. Jones, E. Mahieu, J. Notholt, C. Paton-Walsh, U. Raffalski, T. Ridder, M. Schneider, C. Servais, and M. De Mazie`re1 (2012), "Validation of IASI FORLI carbon monoxide retrievals using FTIR data from NDACC", *Atmos. Meas. Tech., 5*, 2751–2761, doi:10.5194/amt-5-2751-2012.
3. NASA DISCOVER-AQ: Deriving Information on Surface Conditions from Column Vertically Resolved Observations Relevant to Air Quality, http://www-air.larc.nasa.gov/missions/discover-aq/discover-aq.html
4. NSF FRAPPE: Front Range Air Pollution and Photochemistry Experiment, https://www2.acom.ucar.edu/frappe
5. M. Van Damme, L. Clarisse, C. L. Heald, D. Hurtmans, Y. Ngadi, C. Clerbaux, A. J. Dolman, J. W. Erisman, and P.-F. Coheur (2014), "Global distributions, time series and error characterization of atmospheric ammonia (NH_3) from IASI satellite observations", *Atmos. Chem. Phys.*, *14*, 2905–2922, doi:10.5194/acp-14-2905-2014.
6. Whitburn, S., M. Van Damme, L. Clarisse, S. Bauduin, C.L. Heald, J. Hadji-Lazaro, D. Hurtmans, M.A. Zondlo, C. Clerbaux, and P.-F. Coheur (2016), "A flexible and robust neural network IASI-NH_3 retrieval algorithm", *J. Geophys. Res.-Atmos.*, *121*, 6581-6599, doi:10.1002/2016JD024828.
7. von Bobrutzki, K., *et al.*, Field inter-comparison of eleven atmospheric ammonia measurement techniques (2010), *Atmos. Meas. Tech., 3*, 91-112.
8. Miller, D.J., K. Sun, L. Tao, J.B. Nowak, Z. Liu, and M.A. Zondlo (2015), "Ammonia and methane dairy emissions in the San Joaquin Valley of California from individual feedlot to regional-scale plumes", *J. Geophys. Res.-Atmos.*, *120*, 9718-9738, doi:10.1002/2015JD023241.
9. Sun, K., L. Tao, M.A. Zondlo, K. Shonkwiler, C. Nash, and J.M. Ham (2015), "Open-path eddy covariance measurements of ammonia fluxes from a beef cattle feedlot", *Agric. Forest Meteorol.*, *213*, 193-202, doi:10.1016/j.agrformet.2015.06.007.